


## Article

# Robust Estimation of Lithium Battery State of Charge with Random Missing Current Measurement Data

Xi Li <sup>1</sup>, Zongsheng Zheng <sup>1,\*</sup>, Jinhao Meng <sup>2</sup>  and Qinling Wang <sup>3</sup><sup>1</sup> College of Electrical Engineering, Sichuan University, Chengdu 610065, China; sugar76@stu.scu.edu.cn<sup>2</sup> School of Electrical Engineering, Xi'an Jiaotong University, Xi'an 710049, China; jinhao@xjtu.edu.cn<sup>3</sup> School of Electrical Engineering, Southeast University, Nanjing 210096, China; qlingwang@seu.edu.cn

\* Correspondence: zongshengzheng@scu.edu.cn; Tel.: +86-15281063498

**Abstract:** The precise estimation of the state of charge (SOC) in lithium batteries is crucial for enhancing their operational lifespan. To address the issue of reduced accuracy in SOC estimation caused by the random missing values of lithium battery current measurements, a joint estimation method which combines recursive least squares with missing input data (MIDRLS) and the unscented Kalman filter (UKF) algorithm is proposed, called the MIDRLS-UKF algorithm. Firstly, the equivalent circuit model of a Thevenin battery is formulated. Then, the current imputation model is designed to interpolate the missing data, based on which the MIDRLS algorithm is derived by solving the unbiased estimation of the gradient of the objective function, thus realizing the online high-precision identification of the circuit model parameters. Furthermore, the proposed algorithm is combined with the UKF algorithm to facilitate the online precise estimation of SOC. The simulation results indicate a marked decrease in the SOC estimation error when employing the proposed joint algorithm, as opposed to the conventional forgetting factor recursive least squares (FFRLS) algorithm combined with the UKF joint estimation algorithm, which verifies the precision and effectiveness of the proposed joint algorithm.

**Keywords:** lithium battery; state of charge estimation; random missing current data; model parameter identification; unscented Kalman filtering



**Citation:** Li, X.; Zheng, Z.; Meng, J.; Wang, Q. Robust Estimation of Lithium Battery State of Charge with Random Missing Current Measurement Data. *Electronics* **2024**, *13*, 4436. <https://doi.org/10.3390/electronics13224436>

Academic Editor: Fabio Corti

Received: 2 October 2024

Revised: 6 November 2024

Accepted: 11 November 2024

Published: 12 November 2024



**Copyright:** © 2024 by the authors. Licensee MDPI, Basel, Switzerland. This article is an open access article distributed under the terms and conditions of the Creative Commons Attribution (CC BY) license (<https://creativecommons.org/licenses/by/4.0/>).

## 1. Introduction

Over the past few years, in order to promote sustainable energy development and the development of a green economy, the electric vehicle industry, which has a positive impact on reducing urban carbon emissions, has developed rapidly [1]. Lithium batteries have become a widely used battery technology in the emerging electric vehicle sector [2] due to their elevated energy and power densities, extended service life, low self-discharge and superior energy conversion efficiency [3]. These attributes render lithium batteries an ideal choice for powering the next generation of electric vehicles, aligning with the global shift towards cleaner and more sustainable transportation options. It is therefore essential to monitor battery status using an effective and precise battery management system (BMS) [4]. Among the various functionalities of a BMS, the estimation of the state of charge (SOC) stands out as particularly crucial. The accurate completion of SOC estimation can show the remaining capacity of the battery, which is essential for preventing overcharging and overdischarging scenarios. By doing so, it ensures the reliable operation of electric vehicles, optimizes the battery's performance, and significantly extends its operational lifespan [5].

SOC estimation methods can be broadly categorized into four groups: methods based on the physical characteristics of the battery, methods based on battery models, data-driven approaches and fusion methods [6]. Among them, the methods based on the physical characteristics of batteries, including the open-circuit voltage method, the internal resistance method and the alternating current impedance method, face challenges in achieving the

accurate estimation of SOC online. These challenges arise from the longer experimental time, higher requirements for experimental conditions and larger errors [7].

The data-driven approach to SOC estimation is centered on the utilization of machine learning algorithms to process extensive datasets of measurement samples and to discern underlying patterns and features within the data. It harnesses the computational capabilities of machine learning to analyze and learn from the complex relationships present in large volumes of battery performance data, thereby enabling the estimation of SOC. There are three predominant types of deep neural networks that are frequently utilized in research, including fully connected neural networks, recurrent neural networks and convolutional neural networks [8]. In addition, in the last few years, a variety of other neural networks have been developed by researchers to enhance the precision and applicability of SOC estimation. For instance, a random search optimization-based Long Short-Term Memory (RS-LSTM) neural network was proposed for precise SOC estimation [9], which is based on the CALCE dataset and a random search algorithm to optimize its performance. Although this kind of method has high flexibility with high estimation accuracy, it is contingent upon the quality of the dataset, entails substantial time investments for model training, and is often characterized by limited robustness [10]. In terms of fusion methods, the researchers in [11] fused neural networks and equivalent circuit models, thus achieving the accurate estimation of SOC over a wide range of temperature conditions. In addition, the researchers in [12] achieved lightweight SOC estimation through EIS data and the equivalent circuit model, which do not require time-consuming model training.

Considering the accuracy, cost, real-time capabilities and other factors of various estimation techniques, the current battery model-based method has a better prospect of application and development potential [13]. The method that employs an equivalent circuit model has low computational demands, making it particularly amenable to embedded systems designed for online SOC estimation. Battery model-based approaches perform SOC estimation by identifying the parameters of the circuit elements within the battery's equivalent circuit model, usually combined with an adaptive filtering algorithm to emulate the battery's dynamic state characteristics [14], such as an extended Kalman filter (EKF), an unscented Kalman filter (UKF) and its improved algorithms [15]. Furthermore, the researchers in [16] proposed a hierarchical adaptive extended Kalman filter (HAEKF) algorithm, which involves the dissection of the second-order RC circuit's state equation model in accordance with the principles of hierarchical identification. Currently, to enhance the timeliness and precision of online model parameter estimation and to address the issue of outdated data accumulation in iterative processes [17], the forgetting factor recursive least square (FFRLS) algorithm is often used to identify model parameters. However, it is only applicable if the input data are complete, i.e., the real-time load current measurements are fully obtained. Should the current detection module in the BMS be faulty, or if the connector is loose or environmental vibrations occur, causing the current measurement value to be missing, this will lead to a large error in the results of parameter identification. These errors can further affect the accuracy of SOC estimation, potentially leading to improper battery usage and jeopardizing the battery's health.

To ensure the high reliability of online battery model parameter identification despite the presence of missing current measurement data, in this paper, we innovatively design a current imputation model to interpolate the missing values of the current. Based on the imputation model, we derive a recursive least squares with missing input data (MIDRLS) algorithm to identify the model parameters by solving the unbiased estimation of the gradient of the objective function. Combining it with the UKF algorithm, we achieve online SOC estimation by using updated model parameters and system states at each cycle.

The remainder of this paper is organized as follows: Section 2 describes the derivation of the MIDRLS algorithm and the model parameter identification process. Section 3 describes the SOC estimation process based on the UKF algorithm and presents the derivation of the MIDRLS algorithm in conjunction with the UKF to perform SOC estimation in real

time. In Section 4, simulation works are conducted to evaluate the performance of the proposed algorithm. Finally, Section 5 presents the discussion and conclusion of the paper.

## 2. Battery Model and Parameter Identification

### 2.1. Battery Model

Equivalent battery models represent the internal state and dynamic characteristics of a battery by forming an equivalent circuit from ideal circuit elements. Prevalent models include the Rint model, Thevenin model, DP model, PNGV model, second-order RC model, etc. [18]. The Thevenin model takes into account the electrochemical reaction inside the battery, which can reflect the polarization characteristics of the battery [19]. It can reflect the actual working characteristics of real lithium batteries, so it is suitable for simulating the performance of lithium batteries. However, its structure is relatively simple and the model parameters are fixed values, so the accuracy is not too high. To precisely reflect the dynamic characteristics of lithium batteries, the Thevenin model [20] was selected for the study in this paper, as shown in Figure 1.

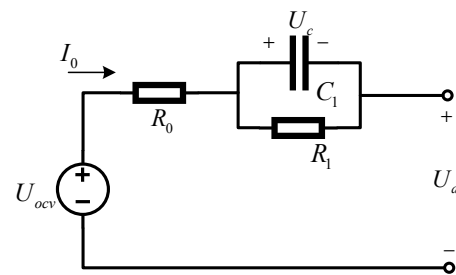


**Figure 1.** Thevenin battery model.

As illustrated in Figure 1, there is an ideal voltage source  $U_{ocv}$ , which denotes the electrical potential of the battery and has a one-to-one correspondence with the SOC of the battery [21]. In addition, it includes a battery equivalent internal resistance  $R_0$ , a polarization resistance  $R_1$  and a polarization capacitor  $C_1$ .  $U_d$  represents the battery terminal voltage and  $I_0$  represents the load current. Therefore,  $R_0$ ,  $R_1$  and  $C_1$  are the parameters that need to be identified.

The model equations can be constructed from Kirchoff's law:

$$\begin{cases} dU_c/dt = -U_c/R_1C_1 + I_0/C_1 \\ U_d = U_{ocv} - U_c - I_0R_0 \end{cases} \quad (1)$$

The values of the model parameters  $R_0$ ,  $R_1$  and  $C_1$  are influenced by factors such as environmental changes, the operational conditions of the battery and the aging process of the battery [22]. This paper employs the proposed MIDRLS algorithm for model parameter identification. It provides real-time identification of the parameters even when the load current measurements are randomly lost, thus avoiding undesirable effects on the SOC estimation results.

### 2.2. The Proposed MIDRLS Algorithm

To enable the capability to accurately identify the model parameters despite the presence of missing model input current data, a new parameter identification algorithm is proposed in this paper.

It is posited that the acquired input data with random loss can be modeled as

$$x_{ic}(n) = g(n)x(n), \quad (2)$$

where  $g(n)$  is a random variable obeying Bernoulli's independent homogeneous distribution, which is independent of  $x(n)$ . The probability of  $g(n)$  taking 1 or 0 is  $p$  or  $1 - p$ , respectively.

We interpolated the missing data, i.e., the missing data were reset to the constant  $\alpha$  times of the data available at the previous moment. The process can be described as

$$\tilde{x}(n) = g(n)x(n) + \alpha(1 - g(n))\tilde{x}(n - 1), \tag{3}$$

where  $\tilde{x}(n)$  represents the imputed data.

The objective function of the FFRLS algorithm is the weighted error sum of squares [23]:

$$J(n) = \sum_{i=0}^n \lambda^{n-i} |d(i) - \mathbf{x}^T(i)w(n)|^2 \tag{4}$$

where  $\lambda$  is the forgetting factor,  $d(i)$  is the output data at moment  $i$  and  $w(n)$  is the parameter vector to be identified.

To prevent the parameter estimation update sequence from failing to converge to the objective function's minimum due to the missing data, we used the imputed data sequence  $\{\tilde{x}(n)\}$  to construct an unbiased estimation of the gradient of the objective function.

Considering

$$\nabla \tilde{J}(n) = -2 \sum_{i=0}^n \lambda^{n-i} \tilde{x}(i) [pd(i) - \tilde{x}^T(i)w(n)], \tag{5}$$

we need to obtain an expression for  $\nabla J(n)$  through  $\mathbb{E}[\nabla \tilde{J}(n)]$ . After some mathematical derivation, one obtains

$$\begin{aligned} \mathbb{E}[\nabla \tilde{J}(n)] &= -2 \sum_{i=0}^n \lambda^{n-i} [pd(i)\mathbb{E}(\tilde{x}(i)) - w(n)\tilde{R}_{i,i}] \\ &= p^2 \nabla J(n) - 2 \sum_{i=0}^n \lambda^{n-i} [\alpha p(1 - p)d(i)\mathbb{E}(\tilde{x}(i - 1)) \\ &\quad - \alpha(1 - p)(Y_{i,i-1} - \alpha(1 - p)\tilde{R}_{i-1,i-1})w(n) \\ &\quad - (1 - p)\text{diag}(\tilde{R}_{i,i} + \alpha^2 \tilde{R}_{i-1,i-1} - \alpha Y_{i,i-1})w(n)]. \end{aligned} \tag{6}$$

where  $\tilde{R}_{i,i} = \mathbb{E}(\tilde{x}(i)\tilde{x}^T(i))$  and  $Y_{i,i-1} = \tilde{R}_{i,i-1} + \tilde{R}_{i-1,i}$ .

Letting  $\bar{x}(i) = \tilde{x}(i) - \alpha(1 - p)\tilde{x}(i - 1)$  and  $x'(i) = \tilde{x}(i) - \alpha\tilde{x}(i - 1)$ , respectively, and in combination with Equation (6), one can obtain

$$\begin{aligned} \nabla J(n) &= -\frac{2}{p^2} \left\{ \mathbb{E} \left[ \sum_{i=0}^n \lambda^{n-i} (pd(i) - \bar{x}^T(i)w(n))\bar{x}(i) \right] \right. \\ &\quad \left. + (1 - p)\mathbb{E} \left[ \sum_{i=0}^n \lambda^{n-i} \text{diag}(x'(i)x'^T(i))w(n) \right] \right\} \end{aligned} \tag{7}$$

When solving for  $w(n)$ , the update process of the MIDRLS algorithm can be obtained by recursion and matrix inversion lemmas, as presented in Algorithm 1.

---

**Algorithm 1** The algorithm flow of the proposed MIDRLS

---

**Input:** the data sequence with random missing  $\{x_{ic}(n)\}$ , the obtained output sequence  $\{d(n)\}$ ,  $\alpha > 0$ ,  $\lambda \in (0, 1)$ ,  $p \in [0, 1]$ .

**Initialize:**  $w(0) = 0$ ,  $M(0) = \kappa I$ ,  $\kappa$  is a pretty small number, the imputed data sequence  $\{\tilde{x}(n)\}$ .

**Update:**  $\xi(n) = \lambda^{-1}M(n - 1)(I + \lambda^{-1}X_n M(n - 1))^{-1}X_n$   
 $w(n) = (I - \xi(n))w(n - 1) + \frac{p}{\lambda}(I - \xi(n))M(n - 1)d(n)\bar{x}(n)$   
 $M(n) = \lambda^{-1}[M(n - 1) - \xi(n)M(n - 1)]$

where  $\bar{x}(n) = \tilde{x}(n) - \alpha(1 - p)\tilde{x}(n - 1)$   
 $x'(n) = \tilde{x}(n) - \alpha\tilde{x}(n - 1)$   
 $X_n = \bar{x}(n)\bar{x}^T(n) - (1 - p)\text{diag}(x'(n)x'^T(n))$

**End For**

---

The forgetting factor allows the weight of previous data in parameter identification to be continuously reduced over long periods of time instead of accumulating over time.

Constructing the unbiased estimation reduces the error in identification results caused by the random loss of current measurements.

### 2.3. Parameter Identification of the Battery Model

To identify the parameters of the battery model through the MIDRLS algorithm, after rewriting Equation (1) in discrete form and letting  $E_k = U_{d,k} - U_{ocv,k}$ , one can obtain the differential equations for the model

$$E_k = \delta_1 E_{k-1} + \delta_2 I_{0,k} + \delta_3 I_{0,k-1} \tag{8}$$

$$U_{d,k} = U_{ocv,k} - I_{0,k}R_0 - U_{c,k}, \tag{9}$$

where

$$\begin{cases} \delta_1 = \varphi \\ \delta_2 = -R_0 \\ \delta_3 = (\varphi - 1)R_1 + \varphi R_0 \end{cases} . \tag{10}$$

$T_0$  is the sampling time,  $\varphi = \exp(-T_0/R_1C_1)$ .

Therefore, the battery model parameters can be obtained as

$$\begin{cases} R_1 = -\delta_2 \\ R_0 = (\delta_1\delta_2 + \delta_3)/(\delta_1 - 1) \\ C_1 = (1 - \delta_1)T_0 / \ln(\delta_1)(\delta_1\delta_2 + \delta_3) \end{cases} . \tag{11}$$

$d(k) = E_k$  is the output data at moment  $k$ ,  $x_{ic}(k) = I_{0,k}$  is the input data with random loss and  $\tilde{x}(k) = [E_{k-1} \tilde{I}_{0,k} \tilde{I}_{0,k-1}]^T$  is the imputed input vector at moment  $k$ . Thus, the coefficient vector  $w(n) = \delta = [\delta_1 \delta_2 \delta_3]$  can be identified recursively through the MIDRLS algorithm and the battery model parameters at moment  $k$  can be calculated from Equation (11).

## 3. SOC Estimation Based on the Joint MIDRLS-UKF Algorithm

### 3.1. Equations of State and Measurement for the Battery Model

The SOC of the lithium battery is typically calculated as the proportion of the remaining capacity relative to the battery's actual maximum capacity [24], and the SOC can be estimated using the ampere-time integration method

$$SOC(t) = SOC(0) + \frac{1}{Q_0} \int_0^t \eta I_0(t) dt \tag{12}$$

where  $SOC(0)$  is the starting point value of SOC,  $Q_0$  is the battery's maximum capacity and  $\eta$  is the Coulombic efficiency which describes the ratio of discharge capacity (mAh/g) to charge capacity (mAh/g).

After discretizing Equation (12) and combining Equations (8) and (9), the state and measurement equations of the battery model can be written as

$$x_k = \begin{pmatrix} \varphi & 0 \\ 0 & 1 \end{pmatrix} x_{k-1} + \begin{pmatrix} (1 - \varphi)R_1 \\ -T_0/Q_0 \end{pmatrix} I_{0,k-1} + w_k \tag{13}$$

$$U_{d,k} = f(SOC_k) - I_{0,k}R_0 - U_{c,k} + v_k, \tag{14}$$

where  $x_k = (U_{c,k}, SOC_k)^T$  is the state variable,  $f(SOC_k)$  expresses the correspondence between  $U_{ocv}$  and  $SOC_k$  and  $w_k$  and  $v_k$  are the process noise and measurement noise of the system, respectively.

This can be further simplified and expressed as a functional relationship:

$$\begin{cases} x_k = g(x_{k-1}, u_{k-1}) + w_k \\ y_k = h(x_k, u_k) + v_k \end{cases} . \tag{15}$$

### 3.2. SOC Estimation Based on the UKF Algorithm

The Kalman filter algorithm is an algorithm for the optimal state estimation of a linear system, whereas  $f(SOC_k)$  is a nonlinear functional relationship in the measurement equation of the battery model.

The EKF algorithm linearizes the system using a Taylor expansion. The UKF algorithm linearizes the nonlinear system through a traceless transformation [25], which approximates the probability distribution of the system's state variables by obtaining a set of sigma sampling points around the initial estimate, thus obtaining the mean and variance of the estimated quantity. In this process, we do not need to derive and iteratively compute the Jacobi matrix, which improves the estimation accuracy and reduces the computational complexity [26].

The detailed implementation steps of the UKF algorithm are outlined below:

- (1) Initialize:

$$\begin{cases} \hat{x}_0 = \mathbb{E}(x_0) \\ P_0 = \mathbb{E}[(x_0 - \hat{x}_0)(x_0 - \hat{x}_0)^T] \end{cases} \quad (16)$$

where  $\hat{x}_0$  is the estimated value of the initial state and  $P_0$  is the initial error covariance matrix.

- (2) Obtain  $2L + 1$  Sigma points at time  $k - 1$ :

$$\begin{cases} x_{i,k-1} = \hat{x}_{k-1}, i = 0 \\ x_{i,k-1} = \hat{x}_{k-1} + (\sqrt{(L + \varepsilon)P_{k-1}})_i, i = 1, 2, \dots, L \\ x_{i,k-1} = \hat{x}_{k-1} - (\sqrt{(L + \varepsilon)P_{k-1}})_{i-L}, i = L + 1, \dots, 2L \end{cases} \quad (17)$$

where  $L$  is the dimension of the state variable,  $\varepsilon = \mu^2(L + \tau) - L$ , and  $\mu$  serves to regulate the proximity of the sampling point to the mean value, generally  $10^{-2} \leq \mu \leq 1$ .  $\tau$  needs to meet  $\tau \geq 0$ .

The weighting factors are

$$\begin{cases} \omega_i^m = \frac{\varepsilon}{L + \varepsilon}, i = 0 \\ \omega_i^c = \frac{\varepsilon}{L + \varepsilon} + 1 + \beta - \mu^2, i = 0 \\ \omega_i^m = \omega_i^c = \frac{1}{2(L + \varepsilon)}, i = 1, 2, 3, \dots, 2L \end{cases} \quad (18)$$

where  $\beta = 2$  for Gaussian distributed variables,  $\omega_i^m$  is the weighted value of the mean of the sampling points and  $\omega_i^c$  is the weighted value of the error covariance matrices at the sampling points.

- (3) Calculate the forecasted values of the mean and covariance matrix:

$$x_{i,k/k-1} = g(x_{i,k-1}, u_{k-1}), i = 0, 1, \dots, 2L \quad (19)$$

$$\bar{\hat{x}}_k = \sum_{i=0}^{2L} \omega_i^m x_{i,k/k-1}, i = 0, 1, \dots, 2L \quad (20)$$

$$P_{k/k-1} = \sum_{i=0}^{2L} \omega_i^c A_{k/k-1} A_{k/k-1}^T \quad (21)$$

where  $x_{i,k/k-1}$  and  $P_{k/k-1}$  are the predicted value of the state vector and the error covariance matrix at the next moment based on the moment  $k - 1$ , respectively, and  $\bar{\hat{x}}_k$  is the estimated value of the state vector at moment  $k$ . In addition,  $A_{k/k-1} = \bar{\hat{x}}_k - x_{i,k/k-1}$ .

- (4) Update the sigma sample points:

$$\begin{cases} x_{i,k/k-1}^- = \bar{\hat{x}}_k, i = 0 \\ x_{i,k/k-1}^- = \bar{\hat{x}}_k + (\sqrt{(L + \varepsilon)P_{k/k-1}})_i, i = 1, 2, \dots, L \\ x_{i,k/k-1}^- = \bar{\hat{x}}_k - (\sqrt{(L + \varepsilon)P_{k/k-1}})_{i-L}, i = L + 1, \dots, 2L \end{cases} \quad (22)$$

- (5) Calculate the estimated values of the output and the Kalman gain:

$$\begin{cases} y_{i,k/k-1} = h(x_{i,k/k-1}^-) \\ \hat{y}_k = \sum_{i=0}^{2L} \omega_i^m y_{i,k/k-1}, i = 0, 1, \dots, 2L \end{cases} \quad (23)$$

$$L_k = P_{xy,k} P_{y,k}^{-1} \quad (24)$$

$$\begin{cases} P_{xy,k} = \sum_{i=0}^{2L} \omega_i^c (x_{i,k/k-1}^- - \bar{x}_k)(y_{i,k/k-1} - \hat{y}_k)^T \\ P_{y,k} = \sum_{i=0}^{2L} \omega_i^c (y_{i,k/k-1} - \hat{y}_k)(y_{i,k/k-1} - \hat{y}_k)^T \end{cases} \quad (25)$$

where  $L_k$  is the gain matrix.

- (6) Update the state variables and error covariance matrix:

$$\hat{x}_k = \bar{x}_k + L_k(y_k - \hat{y}_k) \quad (26)$$

$$P_k = P_{k/k-1} - L_k P_{y,k} L_k^T \quad (27)$$

where  $y_k = U_{d,k}$  is the actual measured value of the battery terminal voltage at the moment  $k$ .

The above steps are iteratively updated to enable the real-time estimation of SOC.

### 3.3. Implementation Flow of the MIDRLS-UKF Algorithm

The values of the model parameters  $R_0$ ,  $R_1$  and  $C_1$  are affected by a number of factors, including the external environment and the internal state of the battery. The MIDRLS algorithm module can accurately identify the parameters  $R_0$ ,  $R_1$  and  $C_1$  even when charging/discharging currents are incompletely measured. The identified values are passed to the UKF algorithm module, which participates in the formation of the functional relationships of the battery state and measurement equations.

Thus, the UKF algorithm module obtains an estimation of the SOC and returns the corresponding  $U_{ocv,k}$  to the MIDRLS algorithm module from the function  $f(SOC_k)$ , which then calculates it and proceeds to the next moment of parameter identification. As a result, the MIDRLS algorithm and the UKF algorithm jointly realize the battery SOC estimation, with the realization flow structure diagram displayed in Figure 2.

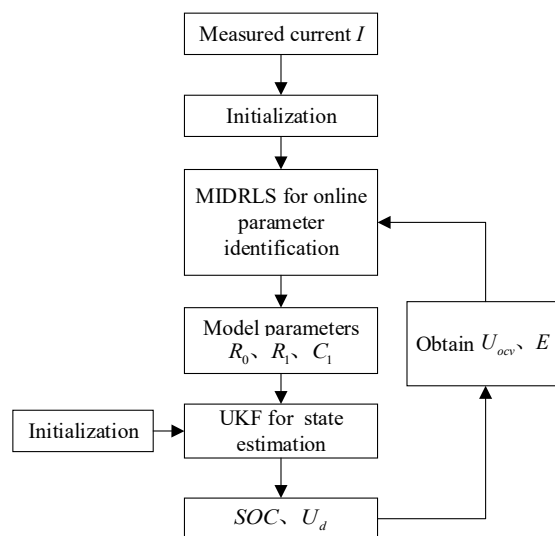


Figure 2. SOC estimation process based on MIDRLS-UKF.



#### 4. Simulation Results and Analysis

In this paper, MATLAB R2022b was used to carry out simulation works to verify the accuracy of the above algorithmic process. The voltage and current data sequences were previously measured. The subject of our tests is the INR 18650-20R battery, with a 2000 mAh capacity, which was charged using a CC-CV protocol at a 1C rate at a test temperature of 25 °C. In the constant current phase, the battery was charged until it reached a terminal voltage of 4.2 V, after which the current gradually decreased to 0.01C in the constant voltage phase. Subsequently, the battery was discharged at a rate of C/20 until the voltage was close to 2.5 V, and then recharged at the same rate until the voltage was nearly 4.2 V to obtain the data used in the simulation works. The value of currents appears to be zero at random moment points, as shown in Figure 3. The curve  $f(SOC_k)$  of the function  $U_{ocv} - SOC$  used in the simulations is derived from the University of Maryland experimental data on OCV incremental testing of INR 18650-20R batteries [27].

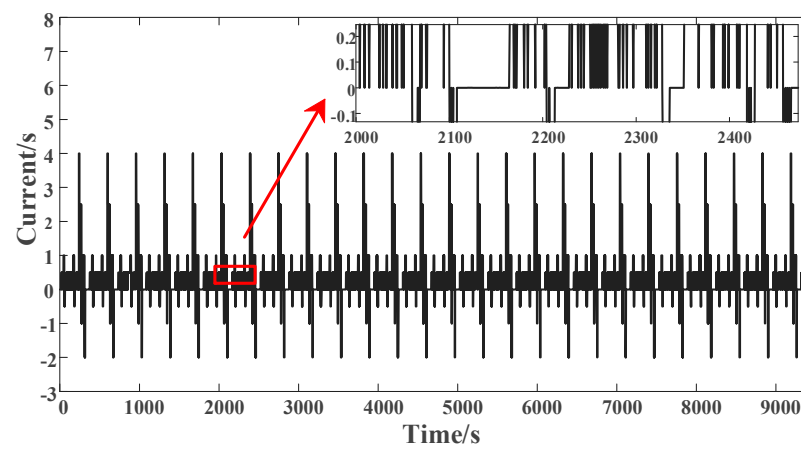


Figure 3. Current measurements with random missing data.

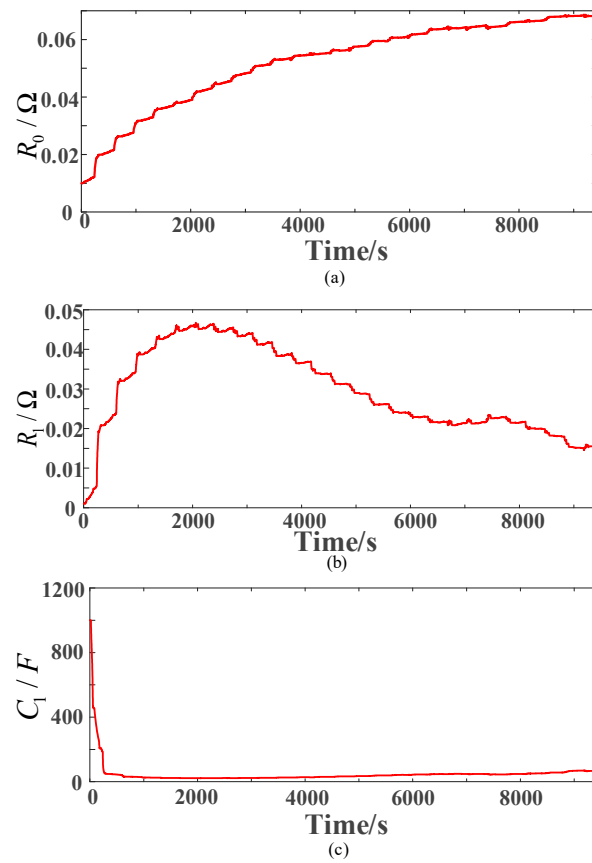
To mitigate the randomness of the experimental outcomes, Monte Carlo simulations were used in the simulations, with a total of 200 runs. The sampling time  $T_0 = 1$  s. The total simulation duration was established at 9434 s and the initial values of the battery equivalent model parameters were set as  $R_0 = 1 \times 10^{-2} \Omega$ ,  $R_1 = 1 \times 10^{-3} \Omega$  and  $C_1 = 1 \times 10^3 F$ . The additional parameters of the algorithm are set in Table 1.

Table 1. Parameters for simulations.

Parameters of the MIDRLS Algorithm	Parameters of the UKF Algorithm
$\lambda = 0.999$	$x_0 = [0 \ 0.8]^T$
$p = 0.8$	$\tau = 0$
$\alpha = 1$	$\mu = 1 \times 10^{-2}$
$M(0) = 0.001 * I$	$\beta = 2$
	$P_0 = [1 \times 10^{-4} \ 0; \ 0 \ 2 \times 10^{-4}]$

Figure 4 shows the outcomes of the MIDRLS algorithm for the real-time identification for the battery model parameters  $R_0$ ,  $R_1$  and  $C_1$ . Overall, the battery’s internal resistance  $R_0$  gradually increases as the SOC decreases, while the polarization resistance  $R_1$  exhibits an initial rise followed by a decline with decreasing SOC. In addition, the polarization capacitance  $C_1$  shows a drastic change in the initial estimation process and then tends to increase progressively alongside a reduction in SOC. The results show that the MIDRLS algorithm enables the real-time correction of the parameter estimates, leading to more accurate SOC state estimation results.





**Figure 4.** Model parameter identification results: (a) battery internal resistance  $R_0$ ; (b) polarization resistance  $R_1$ ; (c) polarization capacitance  $C_1$ .

Subsequently, we conducted a comparative analysis of the estimation outcomes between the MIDRLS-UKF and FFRLS-UKF algorithms under identical simulation conditions. According to the estimation process, it can be seen that based on the identified model parameters, the terminal voltage can be projected using the UKF algorithm. As can be seen in Figure 5, for the MIDRLS algorithm, initial deviations in terminal voltage predictions occur due to the erratic fluctuations in the parameter estimates. However, the accuracy improves over time. Moreover, in general, compared to the FFRLS-UKF algorithm, the terminal voltage estimation results based on the MIDRLS-UKF algorithm are much closer to the actual measured values.

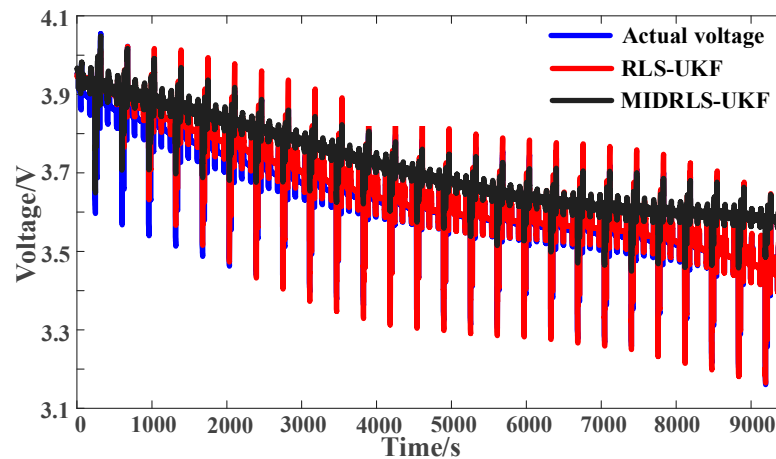


**Figure 5.**  $U_d$  estimation results.

A comparison of the final SOC estimation results is shown in Figure 6. In the presence of random missing current measurements, despite the increased computational demands of the MIDRLS-UKF algorithm over the FFRLS-UKF algorithm, the SOC estimation result curve of MIDRLS-UKF aligns closely with the actual SOC curve very well. It can be inferred that this is because the model parameters estimated by the MIDRLS algorithm turned out to be accurate. However, the FFRLS-UKF algorithm exhibits initial discrepancies in SOC estimation, which are exacerbated over time. This divergence can be attributed to the FFRLS algorithm's failure to converge to the minimum steady state error when the gradient descent is applied in the presence of missing current data.

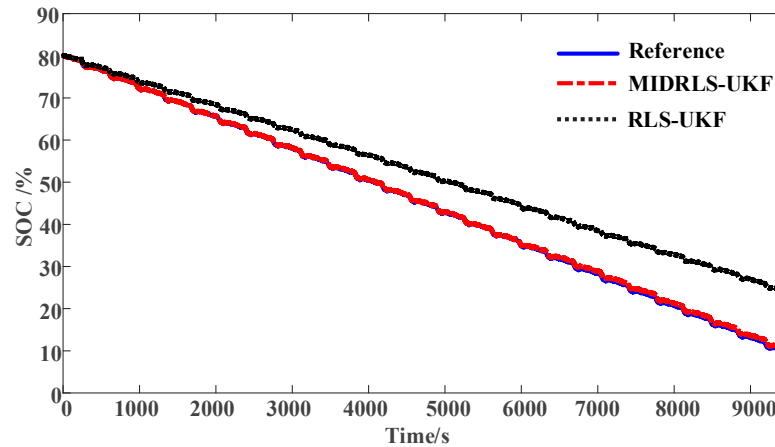


Figure 6. SOC estimation results.

To make the results more intuitive, Figure 7 illustrates the SOC estimation error rates. It is evident that the FFRLS-UKF algorithm experiences a rapid increase in SOC estimation error, whereas the error for the proposed MIDRLS-UKF algorithm remains below 0.05%, indicating a substantial enhancement in accuracy. To further compare the estimation accuracy of the algorithms, we also calculated the root mean square error (RMSE) and the maximum absolute error (MAE) in Table 2. They are defined, respectively, as

$$RMSE = \sqrt{\frac{1}{T} \sum_{i=1}^T (SOC_i - SOC'_i)^2} \quad (28)$$

$$MAE = |SOC_i - SOC'_i|_{\max} \quad (29)$$

where  $SOC_i$  is the actual value of the SOC at moment  $i$  and  $SOC'_i$  is the estimated value of the SOC at moment  $i$ . As presented in Table 2, the MAEs and RMSEs for the MIDRLS-UKF are significantly lower compared to those of the FFRLS-UKF, which verifies the superior estimation accuracy of the proposed algorithm.

Table 2. MSEs and MAEs of SOC estimation methods.

Algorithm	RMSE (%)	MAE (%)
MIDRLS-UKF	0.43%	0.81%
FFRLS-UKF	8.12%	14.64%

Since the initial value of the algorithm is often unknown, we tested the performance of the proposed algorithm against incorrect initial values. SOC estimation was carried out after setting the initial value of SOC to 0.7 and 0.9, respectively, and the outcomes are depicted in Figure 8. The results demonstrate that the MIDRLS-UKF algorithm swiftly rectifies initial value discrepancies, achieving highly accurate SOC estimation with remark-

able stability. This further verifies the exceptional applicability, robustness and reliable estimation performance of the proposed algorithm.

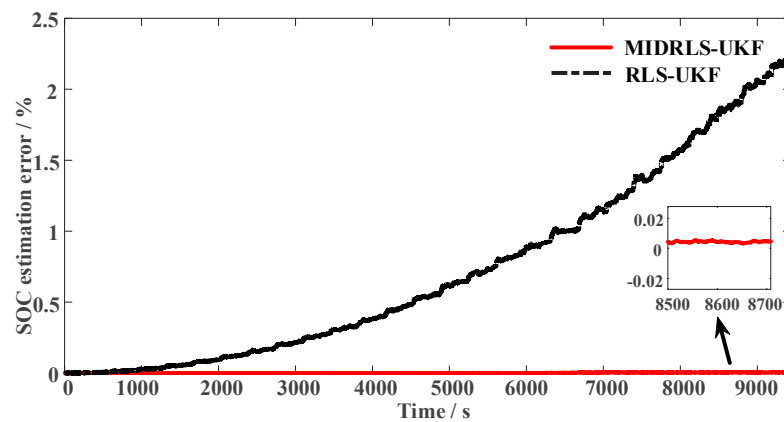


Figure 7. SOC estimation error.

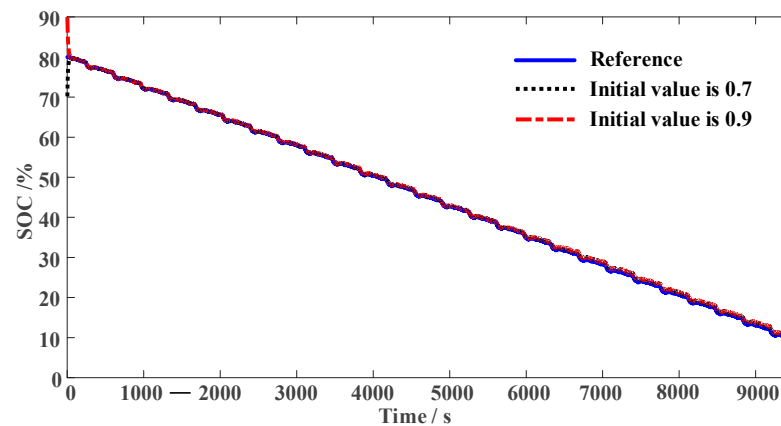


Figure 8. SOC estimation results under inaccurate initial values of MIDRLS-UKF.

## 5. Conclusions

Focusing on the problem that real-time current measurements may be randomly missing during the SOC estimation of lithium batteries, thus impairing estimation precision, this study employs the MIDRLS algorithm to identify the model parameters based on the Thevenin battery model. Concurrently, the UKF algorithm is utilized to estimate the battery state variables, thus enabling the joint estimation of the SOC. The estimation accuracy is then contrasted with those of the conventional joint FFRLS-UKF joint algorithm. The simulation results verify the accuracy of the joint MIDRLS-UKF algorithm proposed in this paper for SOC purposes. The maximum SOC estimation error of the MIDRLS-UKF algorithm does not exceed 0.05%, with the RMSE and MAE of the estimation results being 0.43% and 0.81%, respectively, indicative of excellent estimation accuracy. Compared with the existing estimation methods, the estimation performance, stability and applicability of the proposed algorithm in this paper are significantly enhanced, which further improves the reliability of the BMS.

**Author Contributions:** Conceptualization, X.L. and Z.Z.; methodology, X.L.; software, X.L.; validation, Z.Z. and J.M.; formal analysis, X.L. and Q.W.; investigation, Z.Z. and J.M.; resources, Q.W. and Z.Z.; data curation, X.L. and Q.W.; writing—original draft preparation, X.L.; writing—review and editing, Z.Z.; visualization, X.L.; supervision, Z.Z. and J.M.; project administration, Z.Z.; funding acquisition, Z.Z. and J.M. All authors have read and agreed to the published version of the manuscript.

**Funding:** This research was partially supported by the National Natural Science Foundation of China (62101362) and the Key Research and Development Program of Shaanxi Province (2024GX-YBXM-442).

**Data Availability Statement:** The raw data supporting the conclusions of this article will be made available by the authors on request.

**Acknowledgments:** The authors would like to thank the editor and reviewers for their sincere suggestions for improving the quality of this paper.

**Conflicts of Interest:** The authors declare that this research was conducted in the absence of any commercial or financial relationships that could be construed as potential conflicts of interest.

### Abbreviations

SOC	state of charge
UKF	unscented Kalman filter
EKF	extended Kalman filter
FFRLS	forgetting factor recursive least square
MIDRLS	recursive least square with missing input data
BMS	battery management system
RMSE	root mean square error
MAE	maximum absolute error

### Symbols

$U_{ocv}$	voltage of the ideal voltage source
$R_0$	battery equivalent internal resistance
$R_1$	polarization resistance
$C_1$	polarization capacitor
$U_d$	battery terminal voltage
$I_0$	load current
$g(n)$	Bernoulli random variable
$x(n)$	input data
$x_{ic}(n)$	input data with random missing values
$p$	probability that input data are not missing
$\alpha$	constant times of imputation
$d(i)$	output data
$w(n)$	parameter vector to be identified
$\lambda$	forgetting factor
$J(n)$	objective function of the FFRLS algorithm
$k$	time step index
$T_0$	sampling time
$Q_0$	maximum capacity of the battery
$\eta$	Coulombic efficiency
$x_k$	state vector
$w_k$	process noise
$v_k$	measurement noise
$\omega_i^m$	weighted value of the mean of the sampling points
$\omega_i^c$	weighted value of the error covariance matrices
$x_{i,k/k-1}$	predicted value of the state variable at time instant $k/k-1$
$P_{k/k-1}$	predicted value of the error covariance matrix at time instant $k/k-1$
$\hat{x}_k$	estimated value of the state variable at moment $k$
$L_k$	gain matrix

### References

1. Liu, C.; Liu, W.; Wang, L.; Hu, G.; Ma, L.; Ren, B. A new method of modeling and state of charge estimation of the battery. *J. Power Sources* **2016**, *320*, 1–12. [[CrossRef](#)]
2. Tong, Y.; Zheng, Z.; Fan, W.; Liu, Z. Improved unscented Kalman filter for state of charge estimation of lithium-ion battery with one-step randomly measurement loss and inaccurate noise covariance matrices. *Digit. Signal Process.* **2022**, *131*, 103780. [[CrossRef](#)]
3. Zubi, G.; Dufo-López, R.; Carvalho, M.; Pasaoglu, G. The lithium-ion battery: State of the art and future perspectives. *Renew. Sustain. Energy Rev.* **2018**, *89*, 292–308. [[CrossRef](#)]

4. Singh, S.; More, V.; Batheri, R. Driving Electric Vehicles Into the Future With Battery Management Systems. *IEEE Eng. Manag. Rev.* **2022**, *50*, 157–161. [[CrossRef](#)]
5. Charkhgard, M.; Farrokhi, M. State-of-Charge Estimation for Lithium-Ion Batteries Using Neural Networks and EKF. *IEEE Trans. Ind. Electron.* **2010**, *57*, 4178–4187. [[CrossRef](#)]
6. Qin, P.; Zhao, L. A Novel Transfer Learning-Based Cell SOC Online Estimation Method for a Battery Pack in Complex Application Conditions. *IEEE Trans. Ind. Electron.* **2023**, *71*, 1606–1615. [[CrossRef](#)]
7. Dubarry, M.; Svoboda, V.; Hwu, R.; Liaw, B.Y. Capacity loss in rechargeable lithium cells during cycle life testing: The importance of determining state-of-charge. *J. Power Sources* **2007**, *174*, 1121–1125. [[CrossRef](#)]
8. Tian, J.; Chen, C.; Shen, W.; Sun, F.; Xiong, R. Deep learning framework for lithium-ion battery state of charge estimation: Recent advances and future perspectives. *Energy Storage Mater.* **2023**, *61*, 102883. [[CrossRef](#)]
9. Chai, X.; Li, S.; Liang, F. A novel battery SOC estimation method based on random search optimized LSTM neural network. *Energy* **2024**, *306*, 132583. [[CrossRef](#)]
10. Zhou, X.; Wang, Y.; Shi, Y.; Jiang, Q.; Zhou, C.; Zheng, Z. Deep Reinforcement Learning-Based Optimal PMU Placement Considering the Degree of Power System Observability. *IEEE Trans. Ind. Inform.* **2024**, *20*, 8949–8960. [[CrossRef](#)]
11. Tang, A.; Huang, Y.; Liu, S.; Yu, Q.; Shen, W.; Xiong, R. A novel lithium-ion battery state of charge estimation method based on the fusion of neural network and equivalent circuit models. *Appl. Energy* **2023**, *348*, 121578. [[CrossRef](#)]
12. Buchicchio, E.; De Angelis, A.; Santoni, F.; Carbone, P.; Bianconi, F.; Smeraldi, F. Battery SOC estimation from EIS data based on machine learning and equivalent circuit model. *Energy* **2023**, *283*, 128461. [[CrossRef](#)]
13. Yang, H.; Sun, X.; An, Y.; Zhang, X.; Wei, T.; Ma, Y. Online parameters identification and state of charge estimation for lithium-ion capacitor based on improved Cubature Kalman filter. *J. Energy Storage* **2019**, *24*, 100810. [[CrossRef](#)]
14. Li, X.; Wang, Z.; Zhang, L. Co-estimation of capacity and state-of-charge for lithium-ion batteries in electric vehicles. *Energy* **2019**, *174*, 33–44. [[CrossRef](#)]
15. Shrivastava, P.; Kok Soon, T.; Bin Idris, M.Y.I.; Mekhilef, S.; Adnan, S.B.R.S. Combined State of Charge and State of Energy Estimation of Lithium-Ion Battery Using Dual Forgetting Factor-Based Adaptive Extended Kalman Filter for Electric Vehicle Applications. *IEEE Trans. Veh. Technol.* **2021**, *70*, 1200–1215. [[CrossRef](#)]
16. Wang, D.; Yang, Y.; Gu, T. A hierarchical adaptive extended Kalman filter algorithm for lithium-ion battery state of charge estimation. *J. Energy Storage* **2023**, *62*, 106831. [[CrossRef](#)]
17. Zhang, S.; Guo, X.; Zhang, X. An improved adaptive unscented kalman filtering for state of charge online estimation of lithium-ion battery. *J. Energy Storage* **2020**, *32*, 101980. [[CrossRef](#)]
18. Shrivastava, P.; Soon, T.K.; Idris, M.Y.I.B.; Mekhilef, S. Overview of model-based online state-of-charge estimation using Kalman filter family for lithium-ion batteries. *Renew. Sustain. Energy Rev.* **2019**, *113*, 109233. [[CrossRef](#)]
19. Putra, W.S.; Dewangga, B.R.; Cahyadi, A.; Wahyunggoro, O. Current estimation using Thevenin battery model. In Proceedings of the Joint International Conference on Electric Vehicular Technology and Industrial, Mechanical, Electrical and Chemical Engineering (ICEVT & IMECE), Surakarta, Indonesia, 4–5 November 2015; pp. 5–9.
20. Kwak, M.; Lkhagvasuren, B.; Park, J.; You, J.-H. Parameter Identification and SOC Estimation of a Battery Under the Hysteresis Effect. *IEEE Trans. Ind. Electron.* **2019**, *67*, 9758–9767. [[CrossRef](#)]
21. Pop, V.; Bergveld, H.J.; het Veld, J.O.; Regtien, P.P.L.; Danilov, D.; Notten, P.H.L. Modeling battery behavior for accurate state-of-charge indication. *J. Electrochem. Soc.* **2006**, *153*, A2013. [[CrossRef](#)]
22. Lai, X.; Zheng, Y.; Sun, T. A comparative study of different equivalent circuit models for estimating state-of-charge of lithium-ion batteries. *Electrochim. Acta* **2018**, *259*, 566–577. [[CrossRef](#)]
23. Leung, S.-H.; So, C.F. Gradient-based variable forgetting factor RLS algorithm in time-varying environments. *IEEE Trans. Signal Process.* **2005**, *53*, 3141–3150. [[CrossRef](#)]
24. Piller, S.; Perrin, M.; Jossen, A. Methods for state-of-charge determination and their applications. *J. Power Sources* **2001**, *96*, 113–120. [[CrossRef](#)]
25. Hossain, M.; Haque, M.E.; Arif, M.T. Kalman filtering techniques for the online model parameters and state of charge estimation of the Li-ion batteries: A comparative analysis. *J. Energy Storage* **2022**, *51*, 104174. [[CrossRef](#)]
26. Wang, K.; Feng, X.; Pang, J.; Duan, C.; Li, L. State of charge (SOC) estimation of lithium-ion battery based on adaptive square root unscented kalman filter. *Int. J. Electrochem. Sci.* **2020**, *15*, 9499–9516.
27. Zheng, F.; Xing, Y.; Jiang, J.; Sun, B.; Kim, J.; Pecht, M. Influence of different open circuit voltage tests on state of charge online estimation for lithium-ion batteries. *Appl. Energy* **2016**, *183*, 513–525. [[CrossRef](#)]

**Disclaimer/Publisher’s Note:** The statements, opinions and data contained in all publications are solely those of the individual author(s) and contributor(s) and not of MDPI and/or the editor(s). MDPI and/or the editor(s) disclaim responsibility for any injury to people or property resulting from any ideas, methods, instructions or products referred to in the content.